ASME Journal of Applied Mechanics
Online journal at:
https://asmedigitalcollection.asme.org/appliedmechanics

Periodic Solutions of Wave Propagation in a Strongly Nonlinear Monatomic Chain and Their Novel Stability and Bifurcation Analyses

Bingxu Zhang
Department of Mechanical Engineering,
University of Maryland,
Baltimore County,
1000 Hilltop Circle,
Baltimore, MD 21250
e-mail: bingxuz1@umbc.edu

Weidong Zhu[1]
Department of Mechanical Engineering,
University of Maryland,
Baltimore County,
1000 Hilltop Circle,
Baltimore, MD 21250
e-mail: wzhu@umbc.edu

A modified incremental harmonic balance (IHB) method is used to determine periodic solutions of wave propagation in discrete, strongly nonlinear, periodic structures, and solutions are found to be in a two-dimensional hyperplane. A novel method based on the Hill's method is developed to analyze stability and bifurcations of periodic solutions. A simplified model of wave propagation in a strongly nonlinear monatomic chain is examined in detail. The study reveals the amplitude-dependent property of nonlinear wave propagation in the structure and relationships among the frequency, the amplitude, the propagation constant, and the nonlinear stiffness. Numerous bifurcations are identified for the strongly nonlinear chain. Attenuation zones for wave propagation that are determined using an analysis of results from the modified IHB method and directly using the modified IHB method are in excellent agreement. Two frequency formulae for weakly and strongly nonlinear monatomic chains are obtained by a fitting method for results from the modified IHB method, and the one for a weakly nonlinear monatomic chain is consistent with the result from a perturbation method in the literature. [DOI: 10.1115/1.4066216]

Keywords: nonlinear wave propagation, modified incremental harmonic balance method, Hill's method, strongly nonlinear monatomic chain, periodic solution, stability, bifurcation

1 Introduction

Wave propagation in periodic structures has attracted attention of many researchers throughout history. It can be traced back to the Newton's first attempt to describe sound propagation in air [1]. Early research of wave propagation in periodic structures focused on continuous systems and linear approximations [2]. For linear continuous periodic structures, there are propagation zones and attenuation zones or stop bands. Waves whose frequencies are in propagation zones can propagate without decay, while those whose frequencies are in attenuation zones cannot propagate. Because of attenuation zones, periodic structures can be used as acoustic filters [3,4], waveguides [5,6], diodes [7], and so on [8]. Theories and methods on wave propagation in linear continuous periodic structures are analyzed in detail in Ref. [9].

However, a structure with linear approximations can significantly differ from a real nonlinear structure, and wave propagation in nonlinear structures requires further research. Nonlinear periodic structures exhibit interesting wave propagation properties compared to linear periodic structures, such as nonreciprocal wave propagation [10], tunable band gaps [11], and amplitude-dependent propagation characteristics [12]. Nonreciprocal wave propagation plays an important role in design of metamaterials and it can be used in a wide range of applications, such as optics [13], acoustics [14], and so on [15]. Librandi et al. [16] designed a one-dimensional array of bistable arches where nonreciprocity and reversibility can be independently programed and are not mutually exclusive. Brandenbourger et al. [17] used local control loops to design a robotic metamaterial and widened design in the field of active metamaterials. Wang et al. [18] experimentally demonstrated nonreciprocity in a dynamic one-dimensional phononic crystal with local elastic properties dependent on time. Tunable band gaps can be used to design metamaterials with the filtering property and Gil et al. [19] designed a radio-frequency microelectromechanical tunable metamaterial-based filter. Amplitude-dependent characteristics are widely found in metamaterials. Manimala and Sun [20] investigated amplitude-dependent dynamic responses in acoustic metamaterials and Mashinskii [21] researched amplitude-dependent effects of longitudinal seismic wave propagation in an interhole space. For continuous, weakly nonlinear, periodic structures, Vakakis and King [22] analyzed a monocoupled periodic structure and identified nonlinear attenuation and propagation zones using the method of

[1]Corresponding author.

Contributed by the Applied Mechanics Division of ASME for publication in the Journal of Applied Mechanics. Manuscript received June 26, 2024; final manuscript received August 3, 2024; published online September 10, 2024. Tech. Editor: Pradeep Sharma.

multiple scales (MMS) in space and time. Manktelow et al. [23] used spatial discretization of infinite periodic structures and a perturbation method, and the transfer matrix method [24], to analyze acoustic and electromagnetic wave propagation in nonlinear one-dimensional periodic media, and compared advantages and disadvantages of the two methods. Autrusson et al. [25] employed a perturbation method and a numerical method to analyze the reflection problem of P or R waves at an edge of a homogeneous plate with quadratic nonlinearity. For discrete nonlinear periodic structures, most researchers use continuous nonlinear periodic structures as substitutes, which implies that wavelengths are much larger than the distance between repeating units. However, the substitution fails when the wavelength is relatively small.

Analysis methods for discrete nonlinear periodic structures are reviewed in Ref. [26]. Main methods include the MMS [27,28], the Lindstedt–Poincare (LP) method [12,29], and the incremental harmonic balance (IHB) method [30]. Manktelow et al. [31] used the MMS to analyze interaction of waves in a monatomic chain with cubic nonlinearity, showing that the predictable dispersion behavior broadens design possibilities of tunable metamaterials. Fronk and Leamy [32] applied a high-order MMS to analyze stability and waveform invariance of periodic solutions of both nonlinear monoatomic and diatomic chains. Jiao and Gonella [33] introduced a fast spatio-temporal time scale to execute the MMS and capture the wavenumber shift of a nonlinear monatomic chain under harmonic boundary excitation.

Compared to the MMS, the LP method is simpler and more widely used. Wang and Wang [29] used the LP method to analyze active control effects on nonlinear phononic crystals. Lazarov and Jensen [11] employed both the LP method and a numerical method to investigate wave propagation in a one-dimensional chain with an attached nonlinear local oscillator, finding that the nonlinear behavior can adjust the position of the stop band. Zhou et al. [34] used the spectro-spatial analysis and the LP method to examine wave packet propagation in weakly nonlinear, acoustic metamaterials, demonstrating that spectro-spatial analysis could capture short-wavelength solitary wave information that the LP method could not, which highlighted limitations of the LP method. Chakraborty and Mallik [35] used the LP method to study interaction of two opposing primary waves in semi-infinite or finite chains, finding that this interaction could generate secondary waves.

The LP method and the MMS are both perturbation methods, which can only solve weakly nonlinear and low-dimensional problems, and whose computation requires much algebra and resources. Perturbation methods become invalid for strongly nonlinear problems. The IHB method, developed by Lau and Cheung [36] in 1981, is widely used to solve strongly nonlinear vibration problems. It is a semi-analytical and semi-numerical method by combining the Newton–Raphson procedure and the Galerkin averaging method, and offers high accuracy and low computational cost since it can be implemented by a computer. However, the IHB method requires suitable initial values, can consume substantial computational resources when the number of harmonic terms and dimensions of nonlinear systems are large, and is challenging to use for obtaining solutions at turning points and jump points. To address these issues, the IHB method has undergone 40 years of development [37–42] and has gradually become a mature method.

For wave propagation in discrete, strongly nonlinear, periodic structures, some researchers have used the harmonic balance method and the IHB method to analyze wave propagation properties. Narisetti et al. [43] used the harmonic balance method to study plane wave propagation in strongly nonlinear periodic media, finding the amplitude-dependent dispersion behavior and group velocities. Wang et al. [30] converted the space variable to a time function, merged the time function with the time variable, and transformed the nonlinear wave propagation problem to a time-delay problem, which was solved using the IHB method. Wei et al. [44] used the IHB method to analyze a granular diatomic lattice chain model, discussing influences of system parameters on the band gap property and finding nonreciprocal transmission of the elastic metamaterial. Song and Zhu [45] used the IHB method to analyze wave propagation and its active control in a strongly nonlinear infinite mass-in-mass lattice, investigating effects of nonlinearity, the mass ratio, and different control actions on wave propagation. In the above literature, the influence of the amplitude of wave motion on the strength of nonlinearity is not considered and the amplitude is relatively small. When the amplitude is small and the nonlinear stiffness is large, the above periodic structures can actually be weakly nonlinear. While the harmonic balance method and the IHB method are effective tools for handling strongly nonlinear structures, they may not converge for discrete, strongly nonlinear, periodic structures.

While the IHB method is suitable for analyzing strongly nonlinear vibration problems, wave propagation problems of discrete, strongly nonlinear, periodic structures differ from vibration problems, requiring some adjustments to the IHB method. For wave propagation problems, solutions of the IHB method are found in this work to be in a two-dimensional hyperplane since most systems lack harmonic excitation and damping. With the IHB method, the Jacobian matrix can become singular, and the IHB method may not converge, especially when the amplitude of wave motion and the nonlinear stiffness are both large. Additionally, for strongly nonlinear problems, bifurcation phenomena often occur, making stability analysis crucial. To authors' knowledge, the previous literature does not analyze stability and bifurcations of strongly nonlinear wave propagation problems.

This work presents an improved form of the IHB method to address the issue of periodic solutions in a two-dimensional hyperplane, and analyzes relationships among the frequency, the amplitude, and system parameters in detail, which is a topic that has not been thoroughly examined before. Additionally, a novel method based on the Hill's method is developed to analyze stability and bifurcations of periodic wave solutions of a strongly nonlinear monatomic chain.

The remainder of this paper is organized as follows: the modified IHB method is described in Sec. 2. Stability analysis of periodic solutions is shown in Sec. 3. Detailed analyses of frequency and amplitude curves versus system parameters are described in Sec. 4. Finally, some conclusions are given in Sec. 5.

2 Periodic Solutions of Wave Propagation in a Strongly Nonlinear Monatomic Chain by a Modified Incremental Harmonic Balance Method

The governing equation of the jth particle in a strongly nonlinear monatomic chain is

$$m\ddot{u}^j + f^L(u^{j-n_L},\ldots,u^j,\ldots,u^{j-n_R}) + f^{NL}(u^{j-n_L},\ldots,u^j,\ldots,u^{j-n_R}) = 0 \tag{1}$$

where an overdot denotes a derivative with respect to time t, u_j is the displacement of the jth particle, n_R and n_L are the maximum numbers of its right- and left-sided particles that influence it, and f^L and f^{NL} denote linear and nonlinear restoring forces, respectively. Because of periodicity of the structure, the number j can be set to zero. Then u^{j+i}, where $i=-n_R,\ldots,n_L$, can be rewritten as

$$u^i = u(\omega t - \mu i),\quad i=-n_R,\ -(n_R-1),\ldots,n_L \tag{2}$$

where ω is the propagation frequency, and μ is the propagation constant that is the product of the wavelength and the wavenumber. By introducing the dimensionless time $\tau=\omega t$, Eq. (1) can be rewritten as

$$\omega^2 m u'' + f^L(u^{-n_L},\ldots,u,\ldots,u^{-n_R}) + f^{NL}(u^{-n_L},\ldots,u,\ldots,u^{-n_R}) = 0 \tag{3}$$

where a prime donates a derivative with respect to time τ.

A modified incremental harmonic balance method can be used to obtain a periodic solution of Eq. (3). The first step of the method is

the increment process. By assuming that the system parameter f_0, which can be some system parameter of the structure such as the propagation constant, the linear stiffness, or the nonlinear stiffness, the propagation frequency ω_0, and displacements u_0 and ${u^i}_0$, where $i = -n_L, \ldots, n_R$, are solutions of Eq. (3), neighboring solutions can be expressed as

$$\begin{cases} f = f_0 + \Delta f \\ \omega = \omega_0 + \Delta\omega \\ u = u_0 + \Delta u \\ u^i = {u^i}_0 + \Delta u^i,\ i = -n_L, \ldots, -1, 1, \ldots, n_R \end{cases} \tag{4}$$

where Δf, $\Delta\omega$, Δu, and Δu^i are increments. Substituting Eq. (4) into Eq. (3) and ignoring high-order increments yield

$$\omega_0{}^2 m\Delta u'' + \sum_{i=-n_L}^{n_R} \frac{\partial F}{\partial u^i}\Delta u^i = R - 2\omega_0 m {u_0}''\Delta\omega - \frac{\partial F}{\partial f}\Delta f \tag{5}$$

where $F = f^L + f^{NL}$ and

$$R = -(\omega_0{}^2 m {u_0}'' + F({u_0}^{-n_L}, \ldots, u_0, \ldots, {u_0}^{-n_R})) \tag{6}$$

is a correction term that vanishes if current solutions are exact.

The second step of the method is the harmonic balance process or the Galerkin process. Solutions of Eq. (3) and their increments can be expressed in Fourier series forms

$$\begin{cases} u_0 = \sum_{k=1}^{m} (a_k \cos(k\tau) + b_k \sin(k\tau)) = \mathbf{C}_s\mathbf{A} \\ u_0^i = \sum_{k=1}^{m} (a_k \cos(k(\tau - i\mu)) + b_k \sin(k(\tau - i\mu))) = \mathbf{C}_s^i\mathbf{A},\ i = -n_L, \ldots, -1, 1, \ldots, n_R \\ \Delta u = \sum_{k=1}^{m} (\Delta a_k \cos(k\tau) + \Delta b_k \sin(k\tau)) = \mathbf{C}_s\Delta\mathbf{A} \\ \Delta u^i = \sum_{k=1}^{m} (\Delta a_k \cos(k(\tau - i\mu)) + \Delta b_k \sin(k(\tau - i\mu))) = \mathbf{C}_s^i\Delta\mathbf{A},\ -n_L, \ldots, -1, 1, \ldots, n_R \end{cases} \tag{7}$$

where

$$\mathbf{C}_s = [\cos\tau,\ \cos 2\tau, \ldots,\ \cos m\tau,\ \sin\tau,\ \sin 2\tau, \ldots,\ \sin m\tau] \tag{8}$$

$$\mathbf{C}_s^i = [\cos(\tau + i\mu),\ \cos 2(\tau + i\mu), \ldots,\ \cos m(\tau + i\mu),\ \sin(\tau + i\mu), \sin 2(\tau + i\mu), \ldots,\ \sin m(\tau + i\mu)] \tag{9}$$

$$\mathbf{A} = [a_1, a_2, \ldots, a_m, b_1, b_2, \ldots, b_m]^{\mathrm{T}} \tag{10}$$

$$\Delta\mathbf{A} = [\Delta a_1, \Delta a_2, \ldots, \Delta a_m, \Delta b_1, \Delta b_2, \ldots, \Delta b_m]^{\mathrm{T}} \tag{11}$$

in which the superscript T represents transpose of a matrix or a vector, and $2m$ is the number of harmonic terms. Submitting Eq. (7) into Eq. (1) and applying the Galerkin process to balance harmonic terms yield

$$\begin{aligned} &\int_0^{2\pi} \mathbf{C}_s^{\mathrm{T}} \left(\omega_0^2 m \mathbf{C}_s'' \Delta\mathbf{A} + \sum_{i=-n_L}^{n_R} \frac{\partial F}{\partial u^i} \mathbf{C}_s^i \Delta\mathbf{A} \right) \mathrm{d}\tau \\ &= \int_0^{2\pi} \mathbf{C}_s^{\mathrm{T}} (- (\omega_0{}^2 m {u_0}'' + F({u_0}^{-n_L}, \ldots, u_0, \ldots, {u_0}^{-n_R}))) \mathrm{d}\tau \\ &\quad - \int_0^{2\pi} \mathbf{C}_s^{\mathrm{T}} \left(2\omega_0 m {u_0}''\Delta\omega + \frac{\partial F}{\partial \mu}\Delta\mu \right) \mathrm{d}\tau \end{aligned} \tag{12}$$

Rearranging Eq. (12) in a matrix form yields

$$\mathbf{K}_A\Delta\mathbf{A} = \mathbf{R} - \mathbf{R}_\omega\Delta\omega - \mathbf{R}_f\Delta f \tag{13}$$

where $\mathbf{K}_A$ is a square matrix of $2m$-dimensions, which is given by

$$\mathbf{K}_A = \int_0^{2\pi} \mathbf{C}_s^{\mathrm{T}} \left(\omega_0^2 m \mathbf{C}_s'' + \sum_{i=-n_L}^{n_R} \frac{\partial F}{\partial u^i} \mathbf{C}_s^i \right) \mathrm{d}\tau \tag{14}$$

and $\mathbf{R}$, $\mathbf{R}_\omega$, and $\mathbf{R}_f$ are vectors of $2m \times 1$ dimensions, which are given by

$$\mathbf{R} = \int_0^{2\pi} \mathbf{C}_s^{\mathrm{T}} (- (\omega_0{}^2 m {u_0}'' + F({u_0}^{-n_L}, \ldots, u_0, \ldots, {u_0}^{-n_R}))) \mathrm{d}\tau \tag{15}$$

$$\mathbf{R}_\omega = \int_0^{2\pi} \mathbf{C}_s^{\mathrm{T}} (2\omega_0 m {u_0}'') \mathrm{d}\tau \tag{16}$$

$$\mathbf{R}_f = \int_0^{2\pi} \mathbf{C}_s^{\mathrm{T}} \left(\frac{\partial F}{\partial f} \right) \mathrm{d}\tau \tag{17}$$

The number of unknowns $\mathbf{A}$, ω, and f in Eq. (13) is two more than the number of equations, and f can be prescribed as a control variable. Equation (13) can be transformed to

$$\mathbf{K}_A\Delta\mathbf{A} = \mathbf{R} - \mathbf{R}_\omega\Delta\omega \tag{18}$$

where the number of unknowns $\mathbf{A}$ and ω are one more than the number of equations. The rank of $\mathbf{K} = [\mathbf{K}_A, \mathbf{R}_\omega]$ is $2m - 1$, which is demonstrated in what follows. When $\mathbf{A}$ and ω are solutions of Eq. (18), one notices that

$$\mathbf{K} \begin{bmatrix} \Delta\mathbf{A} \\ \Delta\omega \end{bmatrix} = \mathbf{0} \tag{19}$$

The matrix $\mathbf{K}$ can provide $2m - 1$ independent constraints of unknowns $\mathbf{A}$ and ω and the number of degrees-of-freedom of solutions is the number $2m + 1$ of unknowns $\mathbf{A}$ and ω minus the number $2m - 1$ of constraints or the rank $2m - 1$ of $\mathbf{K}$, which equals 2. Hence, solutions of Eq. (18) are in a two-dimensional hyperplane, as indicated earlier. In order to ensure unique solutions, two Fourier coefficients a_i and b_i should be prescribed, e.g., a_1 and b_1 are assumed to be constant. Equation (18) can be transformed to

$$\mathbf{K}_{\mathrm{A1}}\Delta\mathbf{A}_1 = \mathbf{R} \tag{20}$$

where $\mathbf{K}_{A1} = [\mathbf{R}_\omega, \mathbf{R}_{a_2}, \ldots, \mathbf{R}_{a_m}, \mathbf{R}_{b_2}, \ldots, \mathbf{R}_{b_m}]$ and $\Delta\mathbf{A}_1 = [\Delta\omega, \Delta a_2, \ldots, \Delta a_m, \Delta b_2, \ldots, \Delta b_m]^{\mathrm{T}}$, in which $\mathbf{R}_{a_i}$ (or $\mathbf{R}_{b_i}$) is the corresponding column in $\mathbf{K}_A$ to a_i (or b_i). In Eq. (20), since the number of unknowns of $\Delta\mathbf{A}_1$ is one less than the number of equations, $\Delta\mathbf{A}_1$ can be obtained by the least-square method:

$$\Delta\mathbf{A}_1 = (\mathbf{K}_{\mathrm{A1}}^{\mathrm{T}}\mathbf{K}_{A1})^{-1}\mathbf{K}_{A1}\mathbf{R} \tag{21}$$

which successfully handles the solution in a two-dimensional hyperplane. The solution process starts from guess solutions, and an iteration process is carried out until the norm of the updated residue $\|\mathbf{R}\|$ is less than a permissible error for convergence, which is 10^{-9} in this work. The procedure in which the propagation frequency ω is prescribed as a control variable is similar to the above procedure. The above methods are referred to as the frequency increment method. For the amplitude increment method and the are-length increment method, one can refer to Refs. [37,38].

3 Stability and Bifurcation Analyses of Periodic Solutions

Stability and bifurcation analyses of periodic solutions of nonlinear wave propagation are challenging tasks. This section provides an approximate method to analyze stability and bifurcations of periodic solutions for nonlinear wave propagation. According to the above IHB method, one can obtain periodic solutions of nonlinear wave propagation. Adding the perturbation $\Delta\mathbf{A}$ to the solution $\mathbf{A}$, i.e.,

$$\mathbf{A} = \mathbf{A}_0 + \Delta\mathbf{A} \tag{22}$$

where $\Delta\mathbf{A}$ is a vector function of the time variable τ, one can subsequently express u and u^i as

$$\begin{cases} u = u_0 + \mathbf{C}_s\Delta\mathbf{A} \\ u^i = u_0^i + \mathbf{C}_s^i\Delta\mathbf{A},\ i = -n_L, \ldots, n_R \end{cases} \tag{23}$$

By noting that u_0 satisfies Eq. (1), submitting Eq. (23) into Eq. (1), linearizing Eq. (1) in terms of $\Delta\mathbf{A}$, and ignoring high-order terms of $\Delta\mathbf{A}$ yield

$$\omega_0^2 m(\mathbf{C}_s\Delta\mathbf{A}'' + 2\mathbf{C}_s'\Delta\mathbf{A}' + \mathbf{C}_s''\Delta\mathbf{A}) + \sum_{i=-n_L}^{n_R}\frac{\partial F}{\partial u^i}\mathbf{C}_s^i\Delta\mathbf{A} = 0 \tag{24}$$

Using the Galerkin process to balance harmonic items yields

$$\int_0^{2\pi}\mathbf{C}_s^T\left(\omega_0^2 m(\mathbf{C}_s\Delta\mathbf{A}'' + 2\mathbf{C}_s'\Delta\mathbf{A}' + \mathbf{C}_s''\Delta\mathbf{A}) + \sum_{i=-n_L}^{n_R}\frac{\partial F}{\partial u^i}\mathbf{C}_s^i\Delta\mathbf{A}\right)d\tau = 0 \tag{25}$$

Rearranging Eq. (25) in a matrix form yields

$$\mathbf{K}_2\Delta\mathbf{A}'' + \mathbf{K}_1\Delta\mathbf{A}' + \mathbf{K}_0\Delta\mathbf{A} = 0 \tag{26}$$

where K_0, K_1, and K_0 are matrices of $2m$-dimensions, which are given by

$$\mathbf{K}_2 = \int_0^{2\pi}\omega_0^2\mathbf{C}_s^{\mathrm{T}}m\mathbf{C}_s\,\mathrm{d}\tau \tag{27}$$

$$\mathbf{K}_1 = \int_0^{2\pi}2\omega_0^2\mathbf{C}_s^{\mathrm{T}}m\mathbf{C}_s\,\mathrm{d}\tau \tag{28}$$

$$\mathbf{K}_0 = \int_0^{2\pi}\mathbf{C}_s^{\mathrm{T}}\left(\omega_0^2 m\mathbf{C}_s'' + \sum_{i=-n_L}^{n_R}\frac{\partial F}{\partial u^i}\mathbf{C}_s^i\right)\mathrm{d}\tau \tag{29}$$

Equation (29) can be changed to the first-order form

$$\mathbf{Y}' = \mathbf{Q}\mathbf{Y} \tag{30}$$

where

$$\mathbf{Y} = \begin{bmatrix}\Delta\mathbf{A} \\ \Delta\mathbf{A}'\end{bmatrix} \tag{31}$$

$$\mathbf{Q} = \begin{bmatrix}\mathbf{0} & \mathbf{I} \\ -\mathbf{K}_2^{-1}\mathbf{K}_0 & -\mathbf{K}_2^{-1}\mathbf{K}_1\end{bmatrix} \tag{32}$$

The solution of Eq. (32) is

$$\mathbf{Y} = e^{\mathbf{Q}\tau}\mathbf{Y}_0 \tag{33}$$

where $\mathbf{Y}_0 = \begin{bmatrix}\Delta\mathbf{A}_0^{\mathrm{T}} & \Delta(\mathbf{A}_0')^{\mathrm{T}}\end{bmatrix}^{\mathrm{T}}$ is an initial value. According to the Hill's method, in order to avoid repetition of solutions, eigenvalues of $\mathbf{Q}$ with absolute values of their imaginary parts less than one can be used to determine stability and bifurcations of a periodic solution. When real parts of the eigenvalues are less than zero, the solution is stable. When one or more of real parts of eigenvalues are larger than zero, the solution is unstable. When one or more of real parts of eigenvalues are equal to zero and the remaining ones are less than zero, the solution is critically stable. When the real part of some of the eigenvalues becomes positive from zero or a negative value, a bifurcation occurs. It is worth noting that the current methodology does not apply to a Hopf bifurcation. When a Hopf bifurcation occurs, the structure produces a quasi-periodic solution. Since a quasi-periodic solution has two or more incommensurable frequencies, the frequency ω in $u^j(\omega t - \mu)$ cannot be determined; hence, a quasi-periodic solution does not exist in the current model. A new methodology needs to be developed if a quasi-periodic solution exists in a model.

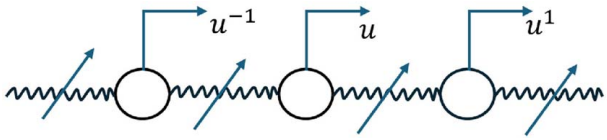

Fig. 1 Schematic of the strongly nonlinear monatomic chain

4 Results and Discussion

For simplicity, only the influence of neighboring cells in the strongly nonlinear monatomic chain is considered, as shown in Fig. 1. The governing equation of a cell particle is simplified to

$$m\ddot{u} + k(2u - u^1 - u^{-1}) + \Gamma(u - u^1)^3 + \Gamma(u - u^{-1})^3 = 0 \tag{34}$$

where k and Γ are the linear stiffness and the cubic nonlinear stiffness of a spring between cells, respectively. With the dimensionless time $\tau = \omega t$ and the linear natural frequency $\omega_0 = \sqrt{k/m}$, Eq. (34) can be transformed to

$$\widetilde{\omega}^2 u'' + (2u - u^1 - u^{-1}) + \widetilde{\Gamma}((u - u^1)^3 + (u - u^{-1})^3) = 0 \tag{35}$$

where $\widetilde{\omega} = \omega/\omega_0$ and $\widetilde{\Gamma} = \Gamma/(m\omega_0^2)$ are the new frequency and the new cubic nonlinear stiffness. According to Eqs. (3)–(13), one can obtain

$$\mathbf{K}_A\Delta\mathbf{A} = \mathbf{R} - \mathbf{R}_{\widetilde{\omega}}\Delta\widetilde{\omega} - \mathbf{R}_\mu\Delta\mu - \mathbf{R}_{\widetilde{\Gamma}}\Delta\widetilde{\Gamma} \tag{36}$$

where the number of unknowns $\mathbf{A}$, $\widetilde{\omega}$, μ, and $\widetilde{\Gamma}$ is three more than the number of equations. Since ω and damping are not present in Eq. (34), the solution of Eq. (36) is in a two-dimensional hyperplane when system parameters μ and $\widetilde{\Gamma}$ are prescribed. One dimension arises because the phase can take any value when the amplitude $A_r = \sqrt{a_1^2 + b_1^2}$ corresponding to the frequency ω is prescribed. The other dimension arises because the amplitude A_r can be any value and is a function of the frequency ω when the phase is prescribed. In order to eliminate the effect of the phase, some Fourier coefficient should be prescribed, e.g., b_1 is assumed to be zero. Additionally, either the amplitude A_r or the frequency ω should be prescribed to ensure a unique solution.

One dimension exists since the frequency ω is not present in Eq. (34). To demonstrate this, when the amplitude A_r and system parameters μ and $\widetilde{\Gamma}$ are prescribed, one chooses Fourier coefficients a_1 and b_1 as control variables. Equation (36) can be transformed to

$$\mathbf{K}_{ab_1}\Delta A_{ab_1} = \mathbf{R} - \mathbf{R}_{\mathrm{A}1}\Delta a_1 - \mathbf{R}_{b1}\Delta b_1 \tag{37}$$

where $\mathbf{K}_{a_1} = [\mathbf{R}_{\widetilde{\omega}}, \mathbf{R}_{a_2}, \ldots, \mathbf{R}_{a_m}, \mathbf{R}_{b_2}, \ldots, \mathbf{R}_{b_m}]$ and $\Delta\mathbf{A}_{a_1} = [\Delta\widetilde{\omega}, \Delta a_2, \ldots, \Delta a_m, \Delta b_2, \ldots, \Delta b_m]^{\mathrm{T}}$. Coefficients a_1 and b_1 keep the amplitude A_r constant and the phase ϕ changing, as shown in Fig. 2(*a*). The frequency curve versus the phase ϕ is a horizontal straight line, as shown in Fig. 2(*b*), indicating that the frequency remains constant. All the points on the curve are critically stable and differ only in the phase, demonstrating that the solution of Eq. (34) is in a one-dimensional hyperplane with respect to the phase when the frequency ω, the amplitude A_r, and system

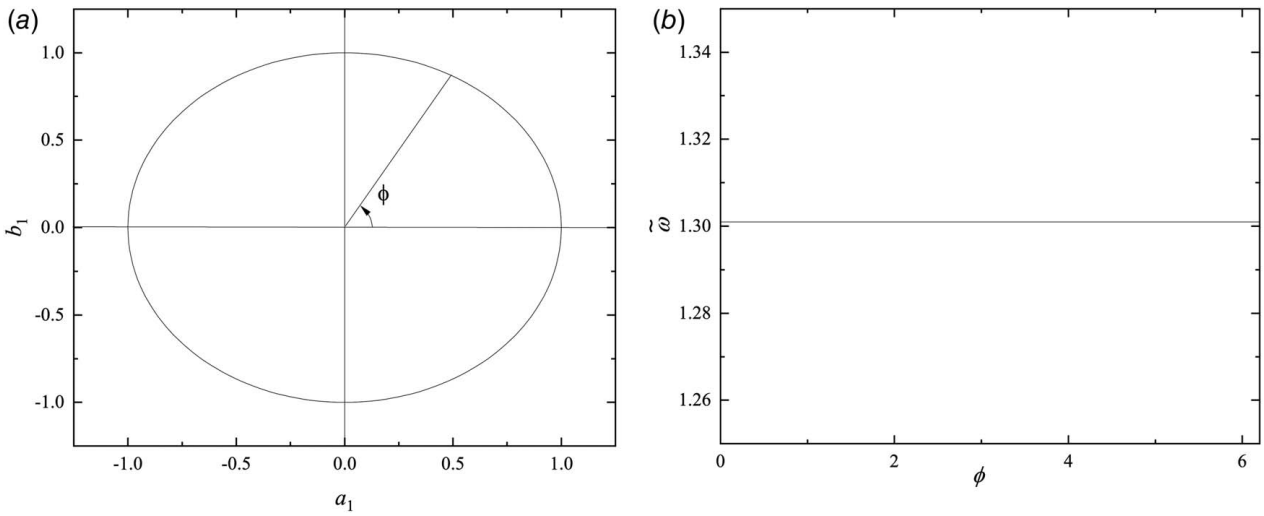

Fig. 2 Solution for wave propagation in the strongly nonlinear monatomic chain with the amplitude $A_r = 1$ and system parameters $\mu = 1$ and $\tilde{\Gamma} = 1$: (*a*) b_1 versus a_1 and (*b*) $\tilde{\omega}$ versus ϕ

parameters μ and $\tilde{\Gamma}$ are prescribed. All the points on the curve have the same stability. Generally speaking, one considers all the points as the same solution, but the influence of the phase must be considered in the solution process of the modified IHB method.

The other dimension exists since damping is not present in Eq. (35). The amplitude A_r can be any positive value and is a function of $\tilde{\omega}$, and all the solutions are critically stable or unstable. When system parameters μ and $\tilde{\Gamma}$ are prescribed, b_1 is assumed to be zero, and $\tilde{\omega}$ is chosen as a control variable, Eq. (36) can be transformed to

$$\mathbf{K}_{\tilde{\omega}}\Delta A_{\tilde{\omega}} = \mathbf{R} - \mathbf{R}_{\tilde{\omega}}\Delta\tilde{\omega} \tag{38}$$

where $\mathbf{K}_{\tilde{\omega}} = [\mathbf{R}_{a_1}, \mathbf{R}_{a_2}, \ldots, \mathbf{R}_{a_m}, \mathbf{R}_{b_2}, \ldots, \mathbf{R}_{b_m}]$ and $\Delta\mathbf{A}_{\tilde{\omega}} = [\Delta a_1, \Delta a_2, \ldots, \Delta a_m, \Delta b_2, \ldots, \Delta b_m]^{\mathrm{T}}$. Frequency curves from the IHB method and the LP method are shown in Fig. 3, where the amplitude A_r corresponding to the frequency ω is the abscissa and $\tilde{\omega}$ is the ordinate. In Fig. 3(*a*), the amplitude and the frequency have a positive correlation, with the bifurcation from the IHB method occurring at the amplitude $A_r = 0.7022$. Eigenvalues near the bifurcation point are shown in Table 1. When the amplitude A_r is zero, the frequency has a positive value, indicating that some part of the frequency depends on the amplitude, while the other part is independent of the amplitude and depends on system parameters. The area A in Fig. 3(*a*) is analyzed in detail in Fig. 3(*b*), where the square of the amplitude A_r is the abscissa and $\tilde{\omega}$ is the ordinate. A straight line from the IHB method appears in Fig. 3(*b*), indicating a linear positive correlation between the square of the amplitude A_r and $\tilde{\omega}$, which can be expressed as

$$\tilde{\omega} - \tilde{\omega}_0 = k_1 A_r^2 \tag{39}$$

where $\tilde{\omega}_0$ is the value of the new frequency when the amplitude A_r is zero, which is a function of system parameters μ and $\tilde{\Gamma}$, and k_1 is also a function of system parameters μ and $\tilde{\Gamma}$. The enlarged figure of the area B in Fig. 3(*a*) is shown in Fig. 3(*c*), where there are two straight lines, indicating that the amplitude A_r and $\tilde{\Gamma}$ have a linear correlation when the amplitude A_r is relatively large, which can be expressed as

$$\tilde{\omega} - \tilde{\omega}_{01} = k_2 A_r \tag{40}$$

where ω_{01} and k_2 are functions of system parameters μ and $\tilde{\Gamma}$. By comparing results from the IHB method and the LP method, one finds that when A_r is small, the difference between results from the IHB method and the LP method is small. As A_r increases, the difference between results from the IHB method and the LP method becomes more pronounced. This discrepancy arises because the LP method is suitable for weak nonlinearity and nonlinearity is strong when A_r is large. Details about the LP method can be referred to Ref. [12]. The correctness of the IHB method and the incorrectness of the LP method for strongly nonlinear wave propagation are verified in what follows.

Figures 2 and 3 show solution curves, indicating that the solution is in a two-dimensional hyperplane when system parameters are prescribed, which means that every point on solution curves has two change directions. When system parameters are prescribed, Eq. (36) can be transformed to

$$\mathbf{K}\Delta\mathbf{A}_p = \mathbf{R} \tag{41}$$

where $\mathbf{K} = [\mathbf{K}_A, \mathbf{R}_{\tilde{\omega}}]$ and $\Delta\mathbf{A}_p = [\Delta\mathbf{A}, \Delta\omega]$. The first six eigenvalues of $\mathbf{K}^{\mathrm{T}}\mathbf{K}$ are shown in Table 2 with two of them being approximately zero when the residue $\mathbf{R}$ is almost $\mathbf{0}$. Two eigenvalue vectors corresponding to two zero eigenvalues are shown in Table 3, representing two change directions of the solution. The component corresponding to $\tilde{\omega}$ in one eigenvector is zero, indicating that the corresponding change direction is caused by the phase, and the component corresponding to $\tilde{\omega}$ in the other eigenvector is not zero, indicating that the corresponding change direction is caused by the absence of damping.

To analyze the relationship between the amplitude A_r and $\tilde{\Gamma}$, $\tilde{\omega}$ and the propagation constant μ should be prescribed, b_1 is assumed to be zero, and $\tilde{\Gamma}$ is chosen as a control variable. Equation (36) can be transformed to

$$\mathbf{K}_{\tilde{\Gamma}}\Delta\mathbf{A}_{\tilde{\Gamma}} = \mathbf{R} - \mathbf{R}_{\tilde{\Gamma}}\Delta\tilde{\Gamma} \tag{42}$$

where $\mathbf{K}_{\tilde{\Gamma}} = [\mathbf{R}_{\tilde{\omega}}, \mathbf{R}_{a_2}, \ldots, \mathbf{R}_{a_m}, \mathbf{R}_{b_2}, \ldots, \mathbf{R}_{b_m}]$ and $\Delta\mathbf{A}_{\tilde{\Gamma}} = [\Delta\tilde{\omega}, \Delta a_2, \ldots, \Delta a_m, \Delta b_2, \ldots, \Delta b_m]^{\mathrm{T}}$. Figure 4 shows the amplitude curve versus $\tilde{\Gamma}$, where the ordinate is the negative second power of the amplitude $\mathbf{A}_r$. A straight line starting from the origin (0, 0) appears in Fig. 4(*a*), which means that the negative second power of the amplitude $\mathbf{A}_r$ and the nonlinear stiffness $\tilde{\Gamma}$ has a direct proportional correlation. The correlation can be expressed as

$$\tilde{\Gamma} = k_2/\mathbf{A}_r^2 \quad \text{or} \quad k_2 = \mathbf{A}_r^2\tilde{\Gamma} \tag{43}$$

where k_2 is a function of the frequency ω and the propagation constant μ; in other words, the product of $\mathbf{A}_r^2$ and the nonlinear stiffness $\tilde{\Gamma}$ is constant when the frequency and the propagation constant are

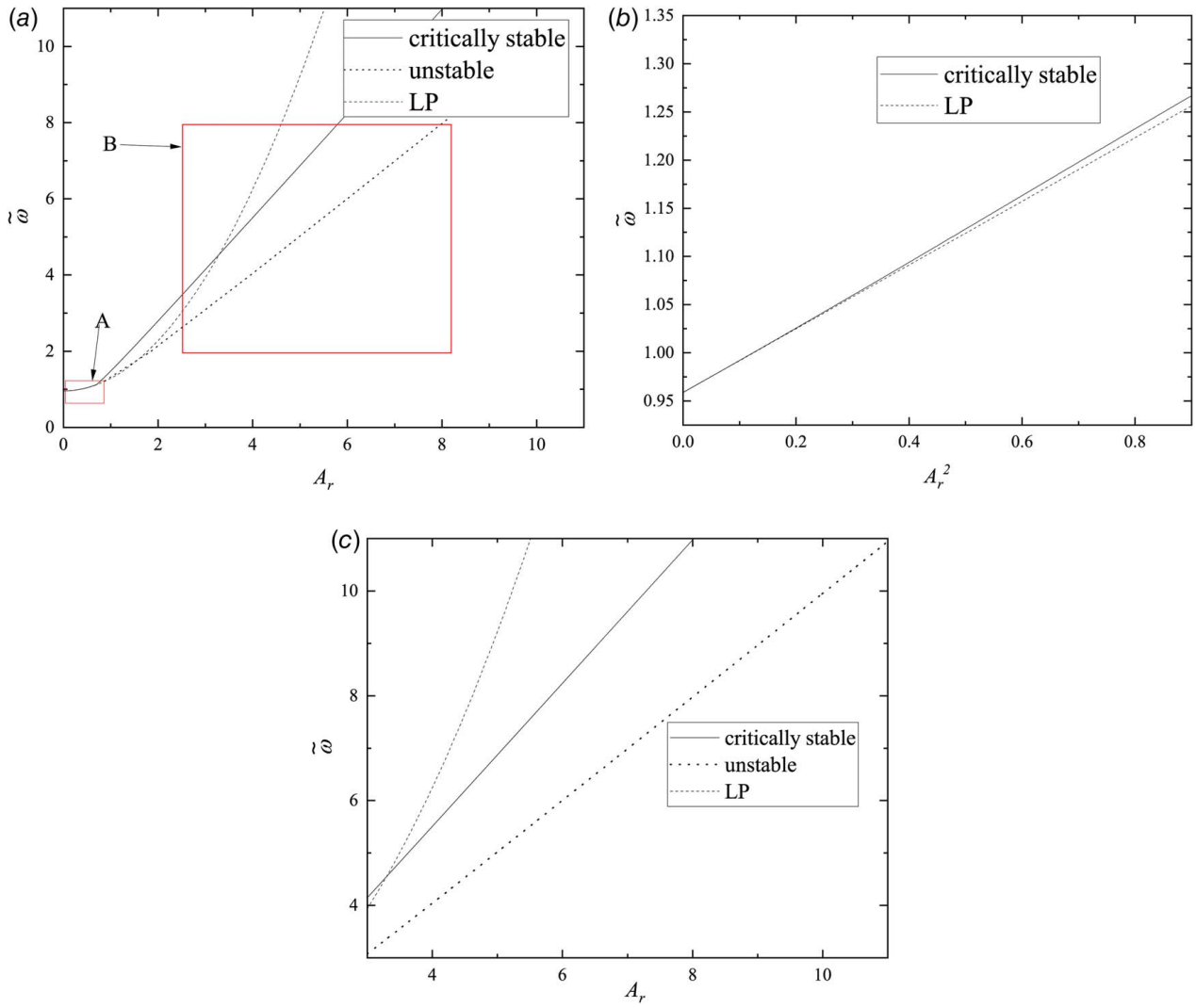

Fig. 3 Frequency curves of $\tilde{\omega}$ for wave propagation in the strongly nonlinear monatomic chain with $\mu = 1$ and $\tilde{\Gamma} = 1$ from the IHB method and the LP method: (*a*) the frequency curve of $\tilde{\omega}$ versus A_r, (*b*) detailed analysis of the area A in (a), and (*c*) the enlarged view of the area B in (a)

prescribed. According to Eq. (43), it is evident that the product of $\mathbf{A}_r^2$ and the nonlinear stiffness $\tilde{\Gamma}$ as a whole influences the frequency. To verify the influence, the frequency curve of $\tilde{\omega}$ versus $\tilde{\Gamma}$ with A_r=1 and that versus $\mathbf{A}_r^2$ with $\tilde{\Gamma}$=1 from the IHB method are the same in Fig. 5 when the propagation constant μ is prescribed. When A_r^2 or $\tilde{\Gamma}$ is small, the difference between results from the IHB method and the LP method is small. When A_r or $\tilde{\Gamma}$ is large, the difference between results from the IHB method and the LP method becomes more pronounced. Two straight lines starting from the origin (0, 0) appear in Figs. 4(*b*) and 4(*c*), where abscissas are the product of $\mathbf{A}_r^3$ and $\tilde{\Gamma}$ and ordinates are the amplitude A_{r2} corresponding to 2ω and the amplitude A_{r3} corresponding to 3ω, respectively. This indicates that the strength of nonlinearity depends more on the amplitude A_r than on $\tilde{\Gamma}$.

To analyze the relationship between the amplitude A_r and the wave propagation constant μ when $\tilde{\Gamma}$ and $\tilde{\omega}$ are prescribed and b_1 is assumed to be zero, Eq. (36) can be transformed to

$$\mathbf{K}_\mu \Delta\mathbf{A}_\mu = \mathbf{R} - \mathbf{R}_\mu \Delta\mu \tag{44}$$

where $\mathbf{K}_\mu = [\mathbf{R}_{a_1}, \mathbf{R}_{a_2}, \ldots, \mathbf{R}_{a_m}, \mathbf{R}_{b_2}, \ldots, \mathbf{R}_{b_m}]$ and $\Delta\mathbf{A}_\mu = [\Delta a_1, \Delta a_2, \ldots, \Delta a_m, \Delta b_2, \ldots, \Delta b_m]^{\mathrm{T}}$. The amplitude curve of A_r

Table 1 Eigenvalues near the bifurcation point of the solution for wave propagation in the strongly nonlinear monatomic chain with system parameters $\mu = 1$ and $\tilde{\Gamma} = 1$

A_r	0.7021	0.7022	0.7023	0.7024
λ_1	0.0000	0.0000	0.0000	0.0000
λ_2	0.0000	0.0000	0.0000	0.0000
λ_3	0.0023i	0.000400i	0.002016	0.0028787
λ_4	−0.0023i	−0.000400i	−0.002016	−0.0028787
λ_5	0.7623i	0.7622960i	0.7622872i	0.7622785i
λ_6	−0.7623i	−0.7622960i	−0.7622872i	−0.7622785i

Table 2 Eigenvalues of $\mathbf{K}^{\mathrm{T}}\mathbf{K}$ for wave propagation in the strongly nonlinear monatomic chain with system parameters $\mu = 1$ and $\tilde{\Gamma} = 1$

Eigenvalue	value
λ_1	0.0000
λ_2	0.0000
λ_3	0.0367
λ_4	1.3100
λ_5	12.8924
λ_6	34.6309

Table 3 Change directions of the solution for wave propagation in the strongly nonlinear monatomic chain with system parameters $\mu = 1$ and $\tilde{\Gamma} = 1$

Variable	Direction 1	Direction 2
a_1	−0.81875	0.00000
a_2	0.00000	0.00000
a_3	0.14499	0.00000
b_1	0.00000	0.97301
b_2	0.00000	0.00000
b_3	0.00000	−0.22997
$\tilde{\omega}$	−0.55543	0.00000

versus the propagation constant μ is shown in Fig. 6, where the amplitude decreases as the propagation constant μ increases, reaching zero at $\mu = 1.42$. It is noteworthy that A_r approaches infinity as μ approaches zero. The bifurcation occurs at $\mu = 1.1$, with eigenvalues near the bifurcation point shown in Table 4.

To analyze the relationship between the frequency ω and the propagation constant μ when $\tilde{\Gamma}$ and the amplitude A_r are prescribed, Eq. (36) can be transformed to

$$\mathbf{K}_{\mu\omega}\Delta\mathbf{A}_{\mu\omega} = \mathbf{R} - \mathbf{R}_{\mu}\Delta\mu \tag{45}$$

where $\mathbf{K}_{\mu\omega} = [\mathbf{R}_{\tilde{\omega}}, \mathbf{R}_{a_2}, \ldots, \mathbf{R}_{a_m}, \mathbf{R}_{b_2}, \ldots, \mathbf{R}_{b_m}]$ and $\Delta\mathbf{A}_{\mu\omega} = [\Delta\tilde{\omega}, \Delta a_2, \ldots, \Delta a_m, \Delta b_2, \ldots, \Delta b_m]^{\mathrm{T}}$. Due to $F(-\mu) = F(\mu)$ and $F(\mu + 2\pi) = F(\mu)$, the frequency curve of $\tilde{\omega}$ versus μ repeats with a period of 2π and is symmetric about $\mu = 0, \pm\pi, \pm 2\pi, \ldots$ Thus, μ can be chosen to range from 0 to π. The frequency curve of $\tilde{\omega}$ versus the propagation constant μ for strongly nonlinear wave propagation and that for linear wave propagation is shown in Fig. 7. In the frequency curve for strongly nonlinear wave propagation, the amplitude A_r is set to one and the nonlinear stiffness $\tilde{\Gamma}$ is also set to one, which are relatively large; this can address the influence of the amplitude A_r on the strength of nonlinearity, which is not considered in the previous literature [43,30,45]. Frequency curves for strongly nonlinear wave propagation from the IHB method and the LP method are shown to be significantly different from that for linear wave propagation, and the difference between frequency curves from the IHB method and the LP method is large. In Fig. 7, the frequency $\tilde{\omega}$ increases with the propagation constant μ. The bifurcation from the IHB method occurs at $\mu = 1.2768$, with eigenvalues near the bifurcation point shown in Table 5.

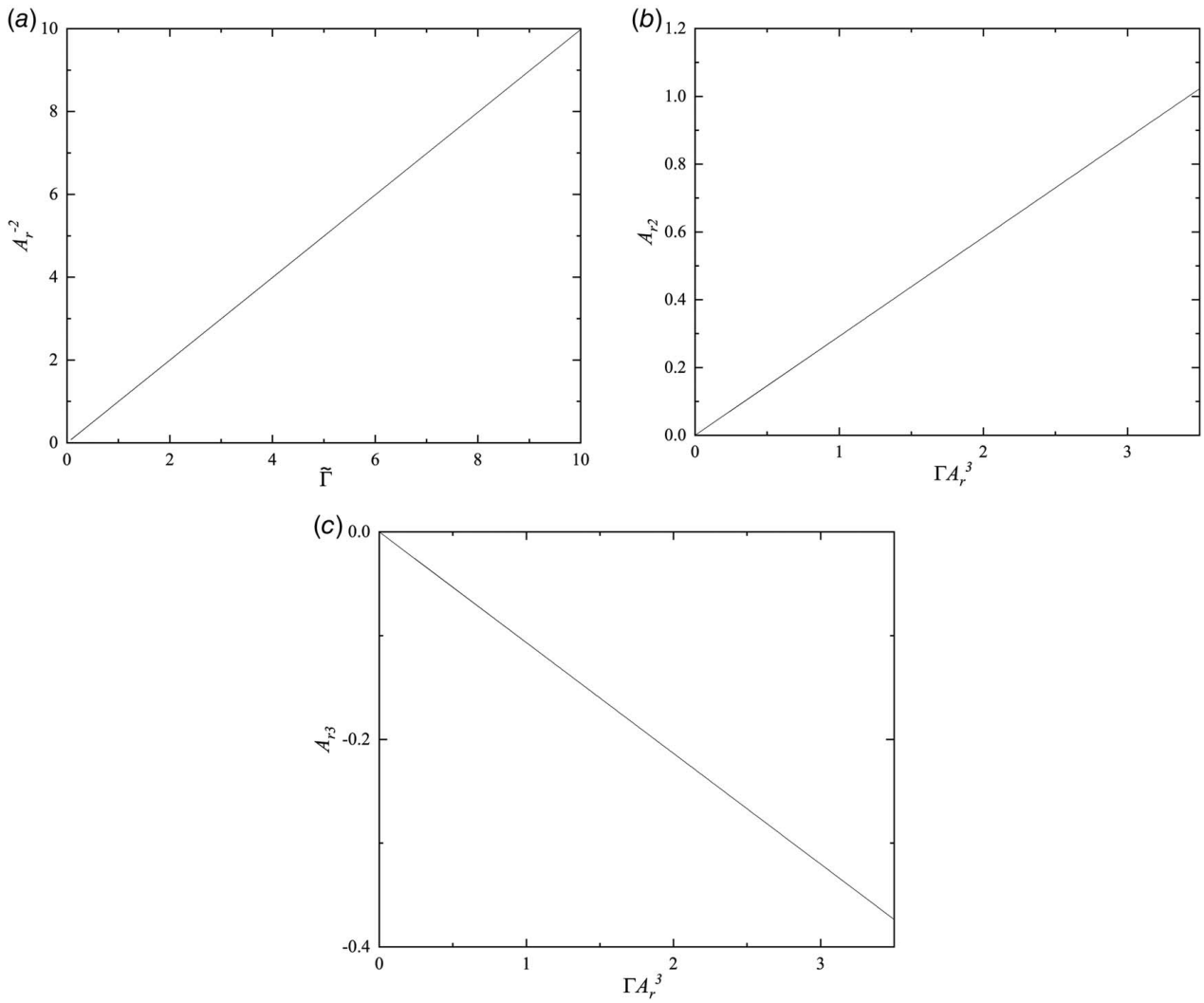

Fig. 4 Amplitude curves for wave propagation in the strongly nonlinear monatomic chain with $\mu = 1$ and $\tilde{\omega} = 1$: (*a*) the curve of the negative second power of the amplitude A_r versus $\tilde{\Gamma}$, (*b*) the curve of the amplitude A_{r2} versus $\tilde{\Gamma}A_r^3$, and (c) the curve of the amplitude A_{r3} versus $\tilde{\Gamma}A_r^3$

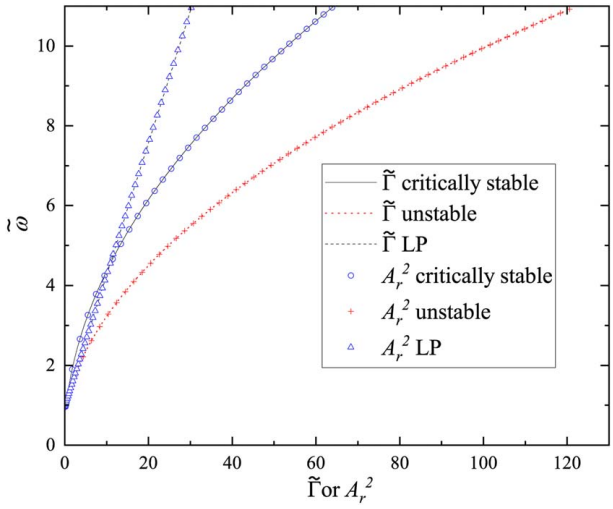

Fig. 5 Frequency curves of $\tilde{\omega}$ for wave propagation in the strongly nonlinear monatomic chain with $\mu = 1$ versus $\tilde{\Gamma}$ with $A_r = 1$ and that versus A_r^2 with $\tilde{\Gamma} = 1$ from the IHB method and the LP method

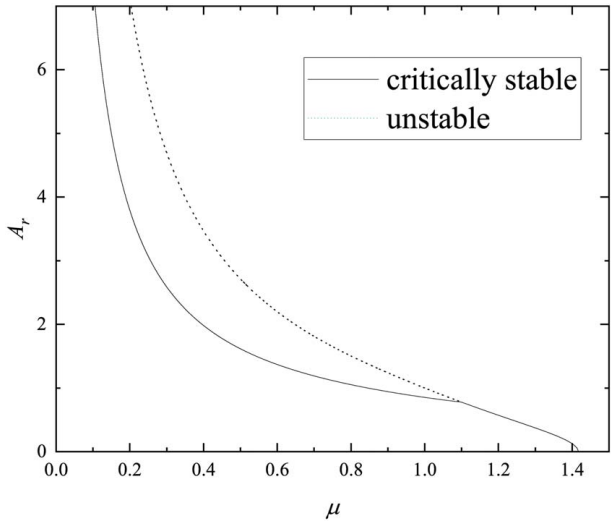

Fig. 6 Amplitude curve of A_r versus μ for wave propagation in the strongly nonlinear monatomic chain with $\tilde{\Gamma} = 1$ and $\tilde{\omega} = 1$

Table 4 Eigenvalues near the bifurcation point of the solution for wave propagation in the strongly nonlinear monatomic chain with system parameters $\tilde{\omega} = 1$ and $\mu = 1$

μ	1.0994	1.0999	1.1003	1.1007
λ_1	0.01027	0.00708	0.00235i	0.00785i
λ_2	−0.01027	−0.00708	−0.00235	−0.00785
λ_3	0.00000	0.00000	0.00000	0.00000
λ_4	0.00000	0.00000	0.00000	0.00000
λ_5	0.92207i	0.92283i	0.92359i	0.92436i
λ_6	−0.92207i	−0.92283i	−0.92359i	−0.92436i

According to Figs. 3 and 6, there exists a region where all the amplitudes are zero, which is called an attenuation zone; it is depicted in Fig. 8, where the abscissa is the propagation constant μ, the ordinate is $\tilde{\omega}$, and the shaded region denotes the attenuation zone. Noting that the product of A_r^2 and $\tilde{\Gamma}$ as a whole influences the frequency ω; the product is zero when A_r is zero, which

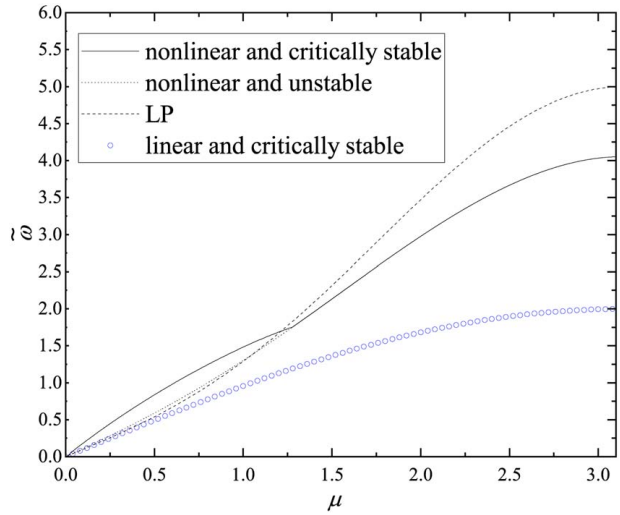

Fig. 7 Frequency curves of $\tilde{\omega}$ versus μ for wave propagation in the strongly nonlinear monatomic chain with $\tilde{\Gamma} = 1$ and $A_r = 1$ and in the linear monatomic chain with $A_r = 1$

Table 5 Eigenvalues near the bifurcation point of the solution for wave propagation in the strongly nonlinear monatomic chain with the amplitude $A_r = 1$ and $\tilde{\Gamma} = 1$

μ	1.2766	1.2767	1.2768	1.2769
λ_1	0.00337	0.002250	0.001117i	0.002750i
λ_2	−0.00337	−0.002250	−0.001117i	−0.002750i
λ_3	0.00000	0.00000	0.00000	0.00000
λ_4	0.00000	0.00000	0.00000	0.00000
λ_5	1.246891i	1.247086i	1.247281i	1.247476i
λ_6	−1.246891i	−1.247086i	−1.247281i	−1.247476i

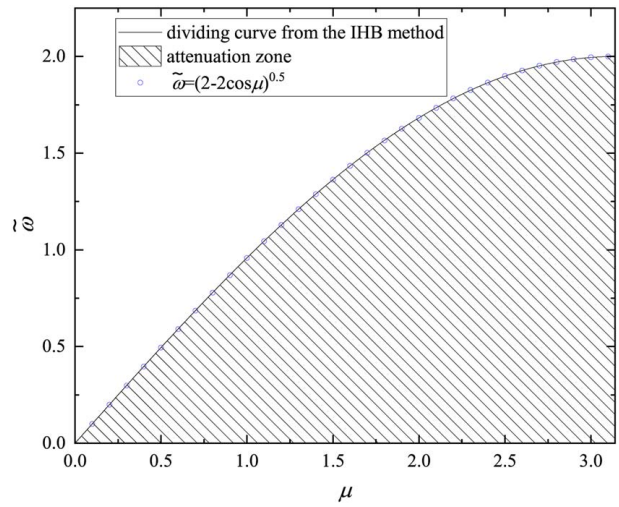

Fig. 8 Attenuation zone of wave propagation in the strongly nonlinear monatomic chain with $\tilde{\Gamma} = 1$

implies that $\tilde{\Gamma}$ has no influence on the frequency when $A_r = 0$. Substituting $u = a_1 \cos\tau$ into the linear equation

$$\tilde{\omega}^2 u'' + (2u - u^1 - u^{-1}) = 0 \tag{46}$$

yields

$$\tilde{\omega}_0 = \tilde{\omega} = \sqrt{2 - 2\cos(\mu)} \tag{47}$$

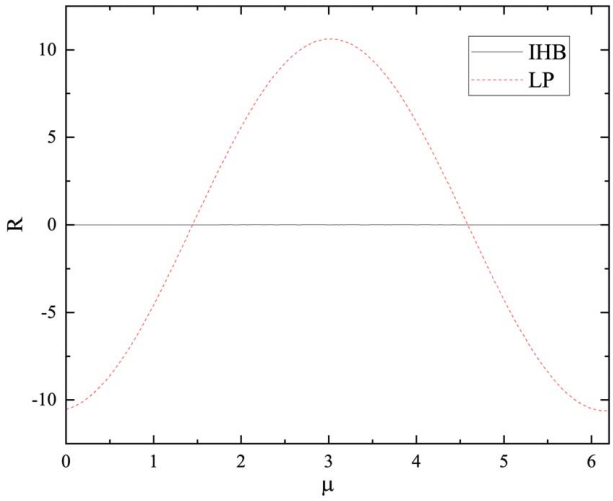

Fig. 9 Comparison of residues of solutions from the IHB method and the LP method for wave propagation in the strongly nonlinear monatomic chain with $\tilde{\Gamma} = 1$, $A_r = 1$, and $\mu = 2$

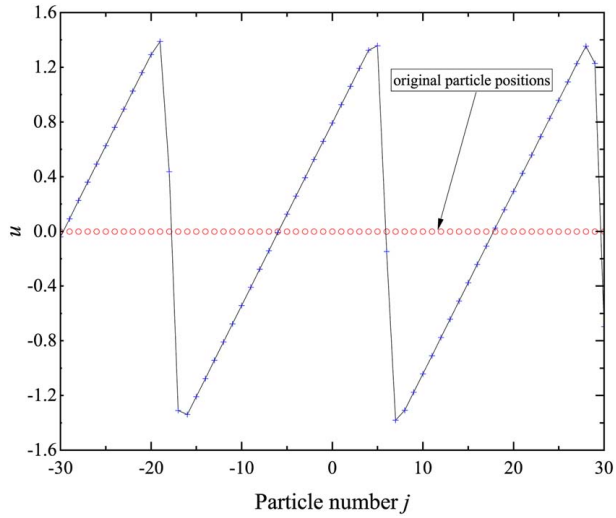

Fig. 11 Periodic wave pattern of a cell in the strongly nonlinear monatomic chain with $\tilde{\Gamma} = 1$, $A_r = 1$, and $\mu = 0.2645$

which serves as the dividing curve of the attenuation zone. The attenuation zone for the strongly nonlinear monatomic chain with $\tilde{\Gamma} = 1$ is under the dividing curve and in excellent agreement with the attenuation zone from the modified IHB method. According to the amplitude-dependent property of wave propagation in the strongly nonlinear monatomic chain in Fig. 3, any point above the attenuation zone is the solution of Eq. (34).

According to Eqs. (39), (42), and (47), when A_r is relatively small, one obtains

$$\widetilde{\omega} = \sqrt{2 - 2\cos(\mu)} + k_2 \tilde{\Gamma} A_r^2 \tag{48}$$

where k_2 is a function of the propagation constant μ, which is consistent with the result in Ref. [12] from a perturbation method. When A_r is relatively large, one obtains

$$\widetilde{\omega} = \widetilde{\omega}_{01} + k_3 \sqrt{\tilde{\Gamma}} A_r \tag{49}$$

where k_3 and $\widetilde{\omega}_{01}$ are functions of μ, and $\tilde{\Gamma} > 0$.

When nonlinearity is weak, the difference between results from both methods is small and the difference is large when nonlinearity is strong. To verify whether results from the IHB method and the LP method are correct or not, solutions from both methods are substituted into Eq. (6) to calculate their residues. Figure 9 shows that the residue from the LP method is significantly larger than that from the IHB method. This indicates that the LP method results in large errors and incorrect results for wave propagation in the strongly nonlinear monatomic chain. In contrast, the IHB method is appropriate for this scenario, yielding minimal errors and correct results. Hence, results from the LP method cannot be used as basis of analysis for wave propagation in the strongly nonlinear monatomic chain. The time history of u versus the dimensionless τ is shown in Fig. 10 and the periodic wave pattern of a cell in the strongly nonlinear monatomic chain is shown in Fig. 11, which describe wave propagation properties.

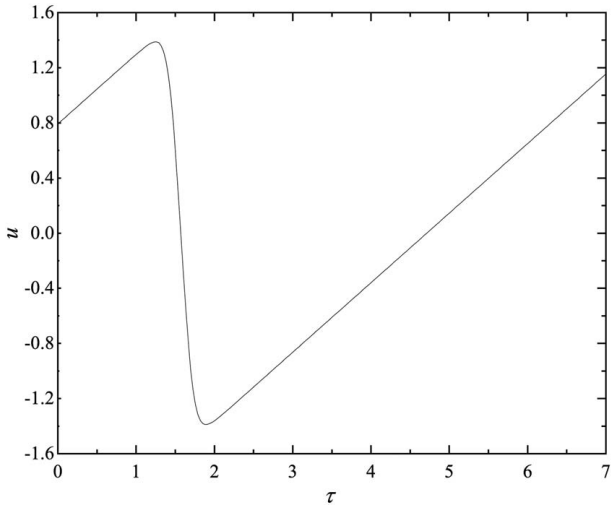

Fig. 10 Periodic response of a cell versus the dimensionless time τ in the strongly nonlinear monatomic chain with $\tilde{\Gamma} = 1$, $A_r = 1$, and $\mu = 0.2645$

5 Conclusion

The modified IHB method proves effective for analyzing wave propagation in discrete, strongly nonlinear, periodic structures. A novel method based on the Hill's method is developed to analyze stability and bifurcations of periodic wave solutions. Detailed analysis of wave propagation in a strongly nonlinear monatomic chain reveals that the solution of the model is in a two-dimensional hyperplane due to the absence of harmonic excitation and damping in it, and the influence of the amplitude of wave motion on the strength of nonlinearity is considered for the strongly nonlinear monatomic chain. The product of the square of the amplitude A_r and $\tilde{\Gamma}$ as a whole influences the frequency. It remains constant when the frequency and the propagation constant are prescribed. The product of the cubic of the amplitude A_r and $\tilde{\Gamma}$ influences coefficients A_{r2} and A_{r3} of high-order harmonic terms, and the strength of nonlinearity of a nonlinear wave propagation problem is reflected more by the amplitude A_r than by $\tilde{\Gamma}$. Attenuation zones of nonlinear wave propagation are successfully identified using an analysis of results from the modified IHB method and directly using the modified IHB method, demonstrating excellent agreement of results from the two methods. Additionally, two formulae for the frequency are derived for weakly and strongly nonlinear monatomic chains using a fitting method, and that for the weakly nonlinear monatomic chain is consistent with the previous finding from a perturbation method.

Acknowledgment

Financial support from the National Science Foundation under Grant No. 2329791 is gratefully acknowledged.

Conflict of Interest

There are no conflicts of interest.

Data Availability Statement

The datasets generated and supporting the findings of this article are obtainable from the corresponding author upon reasonable request.

References

[1] Newton, I., 1686, *Principia–book II, imprimatur S*, Pepys, Reg. Soc. Præses, London.

[2] Wang, K., Liu, Y., and Yang, Q. S., 2015, "Tuning of Band Structures in Porous Phononic Crystals by Grading Design of Cells," Ultrasonics, **61**, pp. 25–32.

[3] Zhu, H. F., and Semperlotti, F., 2013, "Metamaterial Based Embedded Acoustic Filters for Structural Applications," AIP Adv., **3**(9), p. 092121.

[4] Zhang, P., and To, A. C., 2013, "Broadband Wave Filtering of Bioinspired Hierarchical Phononic Crystal," Appl. Phys. Lett., **102**(12), p. 121910.

[5] Kafesaki, M., Sigalas, M. M., and García, N., 2000, "Frequency Modulation in the Transmittivity of Wave Guides in Elastic-Wave Band-Gap Materials," Phys. Rev. Lett., **85**(19), pp. 4044–4047.

[6] Khelif, A., Djafari-Rouhani, B., Vasseur, J., Deymier, P. A., Lambin, P., and Dobrzyński, L., 2002, "Transmittivity Through Straight and Stublike Waveguides in a Two-Dimensional Phononic Crystal," Phys. Rev. B, **65**(17), p. 174308.

[7] Chen, J. J., Zhang, H. B., and Han, X., 2012, "Asymmetric Lamb Wave Propagation in Graded Grating Phononic Crystal Slabs," 2012 Symposium on Piezoelectricity, Acoustic Waves, and Device Applications (SPAWDA), Shanghai, China, Nov. 23–25, pp. 399–401.

[8] Huang, C. Y., Sun, J. H., and Wu, T. T., 2010, "A Two-pPort Zno/Silicon Lamb Wave Resonator Using Phononic Crystals," Appl. Phys. Lett., **97**(3), p. 031913.

[9] Graff, K. F., 2012, *Wave Motion in Elastic Solids*, Dover Publications, New York.

[10] Li, X.-F., Ni, X., Feng, L., Lu, M.-H., He, C., and Chen, Y.-F., 2011, "Tunable Unidirectional Sound Propagation Through a Sonic-Crystal-Based Acoustic Diode," Phys. Rev. Lett., **106**(8), p. 084301.

[11] Lazarov, B. S., and Jensen, J. S., 2007, "Low-Frequency Band Gaps in Chains With Attached Non-linear Oscillators," Int. J. Non-linear Mech., **42**(10), pp. 1186–1193.

[12] Narisetti, R. K., Leamy, M. J., and Ruzzene, M., 2010, "A Perturbation Approach for Predicting Wave Propagation in One-Dimensional Nonlinear Periodic Structures," ASME J. Vib. Acoust., **132**(3), p. 031001.

[13] Xu, H., Jiang, L., Clerk, A., and Harris, J., 2019, "Nonreciprocal Control and Cooling of Phonon Modes in an Optomechanical System," Nature, **568**(7750), pp. 65–69.

[14] Devaux, T., Tournat, V., Richoux, O., and Pagneux, V., 2015, "Asymmetric Acoustic Propagation of Wave Packets Via the Self-demodulation Effect," Phys. Rev. Lett., **115**(23), p. 234301.

[15] Boechler, N., Theocharis, G., and Daraio, C., 2011, "Bifurcation-Based Acoustic Switching and Rectification," Nat. Mater., **10**(9), pp. 665–668.

[16] Librandi, G., Tubaldi, E., and Bertoldi, K., 2021, "Programming Nonreciprocity and Reversibility in Multistable Mechanical Metamaterials," Nat. Commun., **12**(1), p. 3454.

[17] Brandenbourger, M., Locsin, X., Lerner, E., and Coulais, C., 2019, "Non-reciprocal Robotic Metamaterials," Nat. Commun., **10**(1), p. 4608.

[18] Wang, Y., Yousefzadeh, B., Chen, H., Nassar, H., Huang, G., and Daraio, C., 2018, "Observation of Nonreciprocal Wave Propagation in a Dynamic Phononic Lattice," Phys. Rev. Lett., **121**(19), p. 194301.

[19] Gil, I., Martın, F., Rottenberg, X., and De Raedt, W., 2007, "Tunable Stop-Band Filter at Q-Band Based on RF-MEMS Metamaterials," Electron. Lett., **43**(21), pp. 1153–1154.

[20] Manimala, J. M., and Sun, C., 2016, "Numerical Investigation of Amplitude-Dependent Dynamic Response in Acoustic Metamaterials With Nonlinear Oscillators," J. Acoust. Soc. Am., **139**(6), pp. 3365–3372.

[21] Mashinskii, E., 2007, "Amplitude-Dependent Effects of Longitudinal Seismic Wave Propagation in the Interhole Space," Izvestiya Phys. Solid Earth, **43**(8), pp. 683–690.

[22] Vakakis, A. F., and King, M. E., 1995, "Nonlinear Wave Transmission in a Monocoupled Elastic Periodic System," J. Acoust. Soc. Am., **98**(3), pp. 1534–1546.

[23] Manktelow, K., Leamy, M. J., and Ruzzene, M., 2013, "Comparison of Asymptotic and Transfer Matrix Approaches for Evaluating Intensity-Dependent Dispersion in Nonlinear Photonic and Phononic Crystals," Wave Motion, **50**(3), pp. 494–508.

[24] Bethune, D. S., 1991, "Optical Harmonic Generation and Mixing in Multilayer Media: Extension of Optical Transfer Matrix Approach to Include Anisotropic Materials," J. Opt. Soc. Am. B, **8**(2), pp. 367–373.

[25] Autrusson, T. B., Sabra, K. G., and Leamy, M. J., 2012, "Reflection of Compressional and Rayleigh Waves on the Edges of an Elastic Plate With Quadratic Nonlinearity.," J. Acoust. Soc. Am., **131**(3), pp. 1928–1937.

[26] Fronk, M., Fang, L., Packo, P., and Leamy, M. J., 2023, "Elastic Wave Propagation in Weakly Nonlinear Media and Metamaterials: A Review of Recent Developments," Nonlinear Dyn., **111**(12), p. 10709.

[27] Fronk, M. D., and Leamy, M. J., 2019, "Direction-Dependent Invariant Waveforms and Stability in Two-Dimensional, Weakly Nonlinear Lattices," J. Sound Vib., **447**, pp. 137–154.

[28] Narisetti, R. K., Ruzzene, M., and Leamy, M. J., 2011, "A Perturbation Approach for Analyzing Dispersion and Group Velocities in Two-Dimensional Nonlinear Periodic Lattices," ASME J. Vib. Acoust., **133**(6), p. 061020.

[29] Wang, Y. Z., and Wang, Y. S., 2018, "Active Control of Elastic Wave Propagation in Nonlinear Phononic Crystals Consisting of Diatomic Lattice Chain," Wave Motion, **78**, pp. 1–8.

[30] Wang, X. F., Zhu, W. D., and Liu, M., 2020, "SteadyState Periodic Solutions of the Nonlinear Wave Propagation Problem of a One-Dimensional Lattice Using a New Methodology With an Incremental Harmonic Balance Method That Handles Time Delays," Nonlinear Dyn., **100**(2), pp. 1457–1467.

[31] Manktelow, K. L., Leamy, M. J., and Ruzzene, M., 2011, "Multiple Scales Analysis of Wave–Wave Interactions in a Cubically Nonlinear Monoatomic Chain," Nonlinear Dyn., **63**(1–2), pp. 193–203.

[32] Fronk, M. D., and Leamy, M. J., 2017, "Higher-Order Dispersion, Stability, and Waveform Invariance in Nonlinear Monoatomic and Diatomic Systems," ASME J. Vib. Acoust., **139**(5), p. 051003.

[33] Jiao, W. J., and Gonella, S., 2021, "Wavenumber-Space Band Clipping in Nonlinear Periodic Structures," Proc. R. Soc. A, **477**(2251), p. 20210052.

[34] Zhou, W., Li, X., Wang, Y., Chen, W., and Huang, G., 2018, "Spectro-spatial Analysis of Wave Packet Propagation in Nonlinear Acoustic Metamaterials," J. Sound Vib., **413**, pp. 250–269.

[35] Chakraborty, G., and Mallik, A., 2001, "Dynamics of a Weakly Non-linear Periodic Chain," Int. J. Non-Linear Mech., **36**(2), pp. 375–389.

[36] Lau, S. L., and Cheung, Y. K., 1981, "Amplitude Incremental Variational Principle for Nonlinear Vibration of Elastic Systems," ASME J. Appl. Mech., **48**(4), pp. 959–964.

[37] Cheung, Y. K., Chen, S. H., and Lau, S. L., 1990, "Application of the Incremental Harmonic Balance Method to Cubic Non-linearity Systems," J. Sound Vib., **140**(2), pp. 273–286.

[38] Lau, S. L., Cheung, Y. K., and Wu, S. Y., 1982, "Variable Parameter Incrementation Method for Dynamic Instability of Linear and Nonlinear Elastic Systems," ASME J. Appl. Mech., **49**(4), pp. 849–853.

[39] Xu, G. Y., and Zhu, W. D., 2010, "Nonlinear and Time-Varying Dynamics of High-Dimensional Models of a Translating Beam With a Stationary Load Subsystem," ASME J. Vib. Acoust., **132**(6), p. 061012.

[40] Wang, X. F., and Zhu, W. D., 2015, "A Modified Incremental Harmonic Balance Method Based on the Fast Fourier Transform and Broyden's Method," Nonlinear Dyn., **81**(1–2), pp. 981–989.

[41] Huang, J. L., and Zhu, W. D., 2017, "A New Incremental Harmonic Balance Method With Two Time Scales for Quasi-periodic Motions of an Axially Moving Beam With Internal Resonance Under Single-Tone External Excitation," ASME J. Vib. Acoust., **139**(2), p. 021010.

[42] Ju, R., Fan, W., and Zhu, W. D., 2020, "An Efficient Galerkin Averaging-Incremental Harmonic Balance Method Based on the Fast Fourier Transform and Tensor Contraction," ASME J. Vib. Acoust., **142**(6), p. 061011.

[43] Narisetti, R. K., Ruzzene, M., and Leamy, M. J., 2012, "Study of Wave Propagation in Strongly Nonlinear Periodic Lattices Using a Harmonic Balance Approach," Wave Motion, **49**(2), pp. 394–410.

[44] Wei, L. S., Wang, Y. Z., and Wang, Y. S., 2020, "Nonreciprocal Transmission of Nonlinear Elastic Wave Metamaterials by Incremental Harmonic Balance Method," Int. J. Mech. Sci., **173**, p. 105433.

[45] Song, M. T., and Zhu, W. D., 2021, "Elastic Wave Propagation in Strongly Nonlinear Lattices and Its Active Control," ASME J. Appl. Mech., **88**(7), p. 071003.